Turning Characteristics and Control of Submerged and Floating Vehicles

ALLEN G. LINDGREN* AND BRIAN N. BELANGER†
University of Rhode Island, Kingston, R.I.

A nonlinear model that permits determination of both the coursekeeping and turning qualities of a submerged or floating vehicle is developed. Under conditions consistent with observed behavior, vehicle performance is shown to be dominated by a relatively small number of characteristic constants. This simplification permits a tradeoff relation to be developed between turning behavior and the required value of maximum rudder-rate. A velocity-adaptive control law is derived that provides optimal response to step changes in yaw angle for both large and small heading commands.

Nomenclature

A = cross-sectional area
A_R = area of rudder
B = breadth of ship
C_b = block coefficient of ship
c.b. = center of buoyancy
c.g. = center of gravity
g = gravitational acceleration
H = draft of ship
I_x,I_y,I_z = moment of inertia due to vehicle mass about the x, y, and z-axes, respectively
I_{zz} = total virtual moment of inertia about the z-axis $(= I_z - N_{\dot{r}})$
I_{zz}' = dimensionless total virtual moment of inertia about z-axis $(= I_{zz}/\frac{1}{2}\rho A l^3)$
K,M,N = total moment about x, y, and z-axes, respectively
l = length of vehicle
m = mass of vehicle
m_L = longitudinal mass
m_T = transverse mass $(= m - Y_{\dot{v}})$
m_T' = dimensionless transverse mass $(= m_T/\frac{1}{2}\rho A l)$
N_r = $\partial N/\partial r$
$N_{\dot{r}}$ = $\partial N/\partial \dot{r}$
N_β = $\partial N/\partial \beta$
N_{δ_r} = $\partial N/\partial \delta_r$
N' = dimensionless total yaw moment $(= N/\frac{1}{2}\rho A l V^2)$
N_r' = $(\partial N/\partial r)/(\frac{1}{2}\rho A l^2 V)$
$N_{\dot{r}}'$ = $(\partial N/\partial \dot{r})/(\frac{1}{2}\rho A l^3)$
N_β' = $(\partial N/\partial \beta)/(\frac{1}{2}\rho A l V^2)$
N_{δ_r}' = $(\partial N/\partial \delta_r)/(\frac{1}{2}\rho A l V^2)$
p,q,r = components of angular velocity projected along vehicle x, y, and z-axes, respectively
$\dot{p},\dot{q},\dot{r}$ = components of angular acceleration projected along vehicle x, y, and z-axes, respectively
R = vehicle minimum turning radius
t = time
u,v,w = velocity components of vehicle velocity vector **V** projected along vehicle body axes x, y, and z, respectively
V = vehicle velocity
V_a = approach velocity of ship
X,Y,Z = total force along x, y, and z-axes, respectively
X' = dimensionless total force along x-axis $(= X/\frac{1}{2}\rho A A^2)$
x_o,y_o,z_o = inertial coordinates
x,y,z = body coordinates (fixed in vehicle with origin at c.b.)
x_g = distance from c.b. to c.g. on x-axis (+ for c.g. forward of c.b.)
Y_r = $\partial Y/\partial r$
$Y_{\dot{v}}$ = $\partial Y/\partial \dot{v}$
Y_{δ_r} = $\partial Y/\partial \delta_r$
Y_β = $\partial Y/\partial \beta$
Y' = dimensionless total lateral force $(= Y/\frac{1}{2}\rho A V^2)$
Y_r' = $(\partial Y/\partial r)/(\frac{1}{2}\rho A l V)$
$Y'_{\dot{v}}$ = $(\partial Y/\partial v)/(\frac{1}{2}\rho A l)$
Y_{δ_r}' = $(\partial Y/\partial \delta_r)/(\frac{1}{2}\rho A V^2)$
Y_β' = $(\partial Y/\partial \beta)/(\frac{1}{2}\rho A V^2)$
β = sideslip angle measured from the velocity vector **V** to the principal plane of symmetry of the vehicle (x,z)
γ_ψ = heading angle $(= \psi - \beta)$
δ_r = angular displacement of rudder-positive for port deflection
Δ = maximum rudder deflection
ρ = density of sea water
ψ = yaw angle, the Euler angle measured from the vertical plane z_0x_0 to the vertical plane z_0x-positive in the positive sense of rotation about the z axis

Received December 17, 1970; revision received May 25, 1971. The authors wish to thank Daniel B. Cretella for his help in the original development of the turning model, and Haruzo Eda of the Davidson Laboratory for his helpful discussions on the turning properties of surface ships. Portions of the research were performed under Contract N00140-68-C-0447 with the U. S. Naval Underwater Research and Engineering Station, Newport, R. I.
Index Categories: Surface Vessel Systems; Submerged Vessel Systems; Navigation, Control, and Guidance Theory.
* Professor of Electrical Engineering.
† Research Assistant.

Introduction

THE steering performance of a submersible or surface ship is defined in terms of its maneuverability and coursekeeping.[1-3] In both calm water and waves, coursekeeping studies are based on linear dynamic models derived by perturbation techniques. The coefficients for the hydrodynamic forces and moments are obtained experimentally by use of "captive models" whose path is predetermined by the (rotating-arm or planar-motion mechanism) test facility.[4,5] For vehicles maintaining a nearly constant course the resulting mathematical model has successfully provided information on vehicle behavior and the design of autopilots.[3]

Unlike the coursekeeping situation in calm water, a maneuvering ship experiences highly nonlinear hydrodynamic forces and moments with saturation of rudder-rate and rudder position occurring in even modest turns.[6] Approaches to this nonlinear problem include the addition of higher-order hydrodynamic terms in the equations of motion[1,6] and the use of "free-running models" whose behavior in a series of standard maneuvers is evaluated. Two of the most frequently employed maneuvers are the "Z-maneuver" and a rudder sequence from "hard-over to hard-over."[1,2] The Z-maneuver is used to indicate the effect of various design factors (e.g., rudder size) on the vehicle response, while the hard-over to hard-over sequence is generally preferred to test the effect of restricted rudder-rate on the vehicle response.[1]

The hard-over to hard-over maneuver is executed in the following manner: with the vehicle on a straight course the rudder is driven to its maximum angle at a given angular rate and maintained at this position until the change of heading reaches an angle equal to the rudder deflection. The rudder is then driven at the same angular rate to the maximum opposite deflection and maintained at this position. A sample maneuver is shown in Fig. 1a. With the cost of increasing the maximum slewing rate reflected in substantial increases of required power, size, and weight of the steering gear, it is essential to use the minimum rate consistent with the desired obtainable performance. In the past, variations in the characteristic quantities (yaw-angle overshoot, lateral overshoot, and time to second-rudder execution) with rudder-rate have been used to determine the tradeoff of turning performance with rudder-rate. A typical plot of lateral overshoot vs rudder-rate is shown in Fig. 1b, and for this particular situation the minimum value of $2\frac{1}{3}$ deg/sec prescribed by the American Bureau of Shipping Rules for Building and Classing Steel Vessels, the U. S. Coast Guard Marine Engineering Regulations, and the Safety of Life at Sea Convention, is seen to provide reasonable performance. However, this rule is uniformly applied to all vessels and does not take into account vehicle size or maneuverability.[7]

In this paper the basic linear model for coursekeeping studies is modified to include the significant nonlinearities. For a moderately maneuverable vehicle, one whose turning-radius-to-length ratio is above 3 or 4, a simple "turning model" is then developed. This model is used to define vehicle turning characteristics, the required control laws for optimal response to commands in heading, and the tradeoff relations between turning performance and maximum rudder-rate. The results of this study permit the desired rudder-rate and autopilot gains to be determined in terms of elementary vehicle parameters.

Review of the Dynamics of Underwater and Floating Vehicles

The vehicle is considered as a rigid body and the modeling follows Lindgren et al.[6] using the nomenclature, coordinate systems, and sign conventions prescribed for submerged bodies in the Society of Naval Architects and Marine Engineers report of the American Towing Tank Conference.[8] The body axes and the principal axes of inertia coincide, with the origin located at the center of buoyancy (c.b.). When the center of gravity (c.g.) is located at the c.b., the equations of motion assume the form:

$$X = m[\dot{u} + qw - rv] \tag{1a}$$

$$Y = m[\dot{v} + ru - pw] \tag{1b}$$

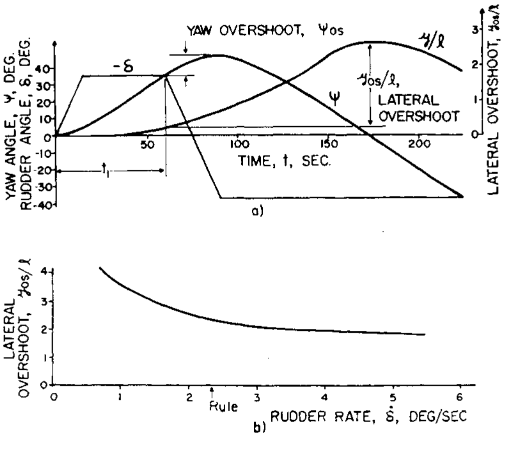

Fig. 1 Typical responses to a hard-over to hard-over rudder sequence; l = 500 ft., V_a = 14.8 knots, A_R/lH = 1.6%. (Courtesy of Eda and Crane[1]).

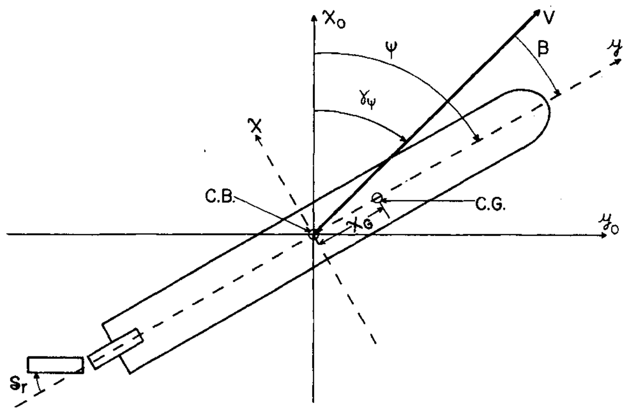

Fig. 2a Submerged vehicle in the azimuth plane.

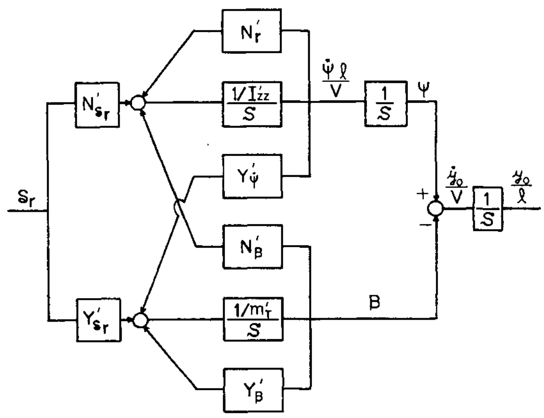

Fig. 2b Block diagram of linear velocity-length normalized azimuth dynamics with nondimensional time, $\lambda = Vt/l$; model derived for coursekeeping conditions.

$$Z = m[\dot{w} + pv - qu] \tag{1c}$$

$$K = I_x\dot{p} + (I_z - I_y)qr \tag{1d}$$

$$M = I_y\dot{q} + (I_x - I_z)rp \tag{1e}$$

$$N = I_z\dot{r} + (I_y - I_x)pq \tag{1f}$$

The hydrodynamic forces (X, Y, and Z) and moments (K, M, and N) are assumed to depend only on nondimensionalized physical variables defined in the nomenclature.

For a vehicle maintaining a nearly constant track, considerable simplification is possible which permits the dominant factors affecting the dynamic response and control of a submerged vehicle to be identified. Under the following assumptions: 1) the vehicle is traveling at a constant speed, 2) roll motion is constrained to negligibly small values by the roll control system, 3) the center of gravity (c.g.) and the center of buoyancy (c.b.) coincide, 4) the (submerged) vehicle is neutrally buoyant, and 5) pitch, yaw, sideslip and attack angles satisfy the conditions of the small angle approximation, only small perturbations occur and the hydrodynamic forces and moments can be represented by the linear (first order) terms of a Taylor expansion about the equilibrium state. This decouples the roll, azimuth, and pitch dynamics. Restricting attention to the azimuth plane results in the set of linear equations:

$$m_T V\dot{\beta} = m_L V\dot{\psi} + Y_\beta\beta + Y_r\dot{\psi} + Y_{\delta_r}\delta_r \tag{2}$$

$$I_{zz}\ddot{\psi} = N_\beta\beta + N_r\dot{\psi} + N_{\delta_r}\delta_r \tag{3}$$

With respect to Fig. 2a, Eqs. (2) and (3) represent, respectively, the summation of forces and moments acting on the hydrodynamic vehicle. The equation for the vehicle lateral

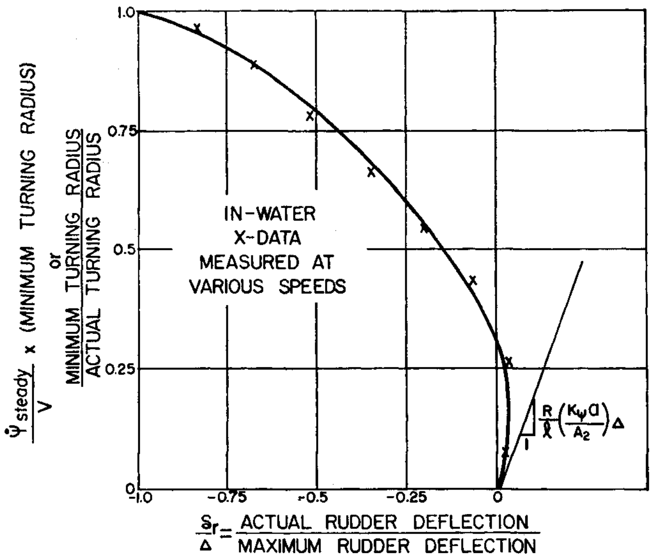

Fig. 3 Normalized (turning-rate)/(rudder-deflection) characteristic for a torpedo-shaped underwater vehicle with unstable body configuration.

displacement is given by

$$\dot{y}_0 = +V\sin(\gamma_\psi) = +V\sin(\psi - \beta) \cong +V(\psi - \beta) \quad (4)$$

where the linearization holds for small values of the heading angle γ_ψ.

Introducing the Laplacian operator s, Eqs. (2–4) become

$$sVm_T\beta = sm_LV\psi + sY_r\psi + Y_\beta\beta + Y_{\delta_r}\delta_r \quad (5)$$

$$s^2I_{zz}\psi = N_\beta\beta + sN_r\psi + N_{\delta_r}\delta_r \quad (6)$$

$$sy_0 = +V(\psi + \beta) \quad (7)$$

The dependency of the coefficients in Eqs. (5–7) on vehicle velocity is removed by use of the nondimensional coefficients and by introducing the velocity-length normalized frequency variable

$$\mathcal{S} = sl/V \quad (8)$$

Equation (8) corresponds to the nondimensional time

$$\lambda = (V/l)t \quad (9)$$

which physically represents the distance traveled along the trajectory in vehicle lengths. Substituting the normalized quantities‡ into Eqs. (5–7) yields

$$\mathcal{S}m_T'\beta = \mathcal{S}Y_{\dot\psi}'\psi + Y_\beta'\beta + Y_{\delta_r}'\delta_r \quad (10)$$

$$\mathcal{S}^2I_{zz}'\psi = N_\beta'\beta + \mathcal{S}N_r'\psi + N_{\delta_r}'\delta_r \quad (11)$$

$$y_0/l = (1/\mathcal{S})(\psi - \beta) \quad (12)$$

where $Y_{\dot\psi}' = m_L/\frac{1}{2}\rho Al + Y_r'$.

A block diagram of the linearized azimuth dynamics is given in Fig. 2b with the corresponding yaw plane transfer functions given in Table 1. Typical values for a torpedo-shaped submersible are given in Table 2. This linear model is the basis of nondimensional coursekeeping studies and autopilot designs for submerged vehicles. For surface ships, the modeling follows the above development with the exception that in the nondimensionalizing process the cross-sectional area A is generally replaced by Hl, where H is the draft of the ship and l its length. Values of the nondimensional coefficients and other parameters for a typical ship[1] are given in Table 3.

‡ The prime (′) denotes the area-length nondimensionalized coefficients defined in the nomenclature.

Table 1 Yaw plane transfer functions

$$\begin{aligned}
\psi/\delta_r &= K_\psi(\mathcal{S} + a)/\mathcal{S}(\mathcal{S}^2 + A_1\mathcal{S} + A_2)\\
K_\psi &= N_{\delta_r}'/I_{zz}'\\
a &= (-Y_\beta' + Y_{\delta_r}'N_\beta'/N_{\delta_r}')/m_T'\\
A_1 &= -(Y_\beta'/m_T') - (N_r'/I_{zz}')\\
A_2 &= (N_r'Y_\beta' - N_\beta'Y_{\dot\psi}')/m_T'I_{zz}'\\
\beta/\delta_r &= K_\beta(\mathcal{S} + b)/(\mathcal{S}^2 + A_1\mathcal{S} + A_2)\\
K_\beta &= Y_{\delta_r}'/m_T'\\
b &= (-N_r' + N_{\delta_r}'Y_{\dot\psi}'/Y_{\delta_r}')/I_{zz}'\\
y_0/\delta_r &= K_\beta(\mathcal{S}^2 + c\mathcal{S} + d)/\mathcal{S}^2(\mathcal{S}^2 + A_1\mathcal{S} + A_2)\\
c &= b - K_\psi/K_\beta\\
d &= -aK_\psi/K_\beta
\end{aligned}$$

Nonlinear Model of Vehicle Dynamics

Tests on actual vehicles (see Fig. 3) demonstrate that the actual steady-state turning characteristic departs significantly from the linear model as the normalized turning rate increases. For example, Fig. 3 shows that an unstable body configuration, which linear modeling predicts should "turn against its rudder" in a steady turn,[9,6] actually "turns with its rudder" for large turning rates. A similar nonlinear characteristic is observed for all vehicles, with the effect being less pronounced as the vehicle body configuration becomes more stable. As seen from the experimental points in Fig. 3, this nonlinearity is in accord with the velocity-length normalized model and defines the maximum vehicle turning rate (or minimum turning radius, R). Since the observed behavior occurs in the normal turning situation, a nonlinear representation for maneuvering vehicles is essential.

One of the prime factors limiting the turning rate is the nonlinear character of the lift force. Typical force and moment vs sideslip angle curves are shown in Fig. 4. To account for this behavior, the Taylor expansion of the hydrodynamic quantities must include the higher-order (or nonlinear) terms.[1,6]

For parametric studies on the turning behavior and control of underwater vehicles, it has been shown[6] that the simplified representation shown in Fig. 5 provides a satisfactory approximation of the nonlinear lift force, where the function $f(\beta_T)$ is selected to closely match the force and moment curves of Fig. 4, X_T is the distance from the c.g. to the tail (where the lift force is assumed to act), and β_T is the sideslip angle measured at the vehicle's tail given by $\beta_T = \beta + X_T\dot\psi/V$. A computer study employing this nonlinear normalized model, with $f(\beta_T)$ approximated by the quadratic $Y_{|\beta_T|\beta_T}'|\beta_T|\beta_T$, resulted in the (steady-state rudder-deflection)/(turning-rate) characteristic shown by the solid curve in Fig. 3. The transient behavior of the nonlinear model, for this "worst case" example of an unstable vehicle indicated close agreement when compared with in-water data for a large signal command in azimuth angle.[6] For moderately maneuverable vehicles, the addition of the above hydrodynamic nonlinearity to the linear perturbation model results in a model that is valid for studying both coursekeeping and turning qualities.

Azimuth Angle Control

The system states potentially available as outputs of the normalized azimuth system are ψ, $l\dot\psi/V$, y_0/l, $\dot{y}_0/V$. If a velocity-adaptive controller is used to generate these system states and linear state feedback employed, then the trajectory required to execute a given command is unaltered by the vehicle velocity. That is, vehicle response is identical in shape for all velocities, although the time required for the maneuver is proportional to l/V. From an alternate viewpoint, when operation is restricted to linear small signal behavior, Eq. (8) indicates that the resulting system bandwidth is proportional to vehicle velocity, a desirable property since the performance requirements of the vehicle generally decrease as vehicle speed decreases.

Table 2 Transfer functions, coefficients, and constants for a typical submerged (symmetric, tail-controlled) vehicle

Nondimensional coefficients		
$N_{\delta_r}' = -0.13$		$N_r' = -0.43$
$Y_{\delta_r}' = -0.27$		$Y_r' = -0.9$
$N_\beta' = 0.6$		$Y_{\dot\psi}' = 0.96$
$Y_\beta' = -2.0$		$m_T' = 3.67$
	$I_{zz}' = 0.191$	
Vehicle constants		
$A = 2.4$ ft^2	$\Delta = 30°$	$l = 18.5$ ft
Transfer functions azimuth plane		
$\delta_r/\psi = -0.693\ (s+0.89)/s(s+0.15)(s+2.65)$		
$\delta_r/\beta = -0.074\ (s+4.67)/(s+0.15)(s+2.65)$		
$y_0/\delta_r = -0.074\ (s+1.37)(s-6.05)/s^2(s+0.15)(s+2.65)$		

For both large and small changes in heading, experiments indicate satisfactory azimuth angle control is realized by a linear control law. This desired velocity-adaptive mode is achieved by letting

$$\delta_c = c_1\psi + c_2(l/V)\dot\psi \tag{13}$$

where δ_c is the actuator input signal, and c_1 and c_2 are feedback constants whose values are determined later in the paper.

Simplified Azimuth Model

Parametric determination of the controller constants appearing in Eq. 13 requires a simplification of the derived nonlinear model that is in agreement with observations of simulated behavior in large heading-change maneuvers. Analytically, the model of Fig. 5 is reduced by first assuming that $N_{\delta_r}'/Y_{\delta_r}' \cong x_T/l \triangleq x_T'$, an assumption very nearly satisfied in torpedo-shaped submersibles. Using the transfer functions defined in Table 1, the above assumption results in the yaw angle control model shown in Fig. 6a where

$$K_{\beta_T} = K_\beta + x_T'K_{\dot\psi} \tag{14}$$

$$a_T = (ax_T'K_{\dot\psi} + bK_\beta)/K_\beta \tag{15}$$

$$a_1 = A_1/2 + [(A_1/2)^2 - A_2]^{1/2} \tag{16}$$

and

$$\epsilon = A_1/2 - [(A_1/2)^2 - A_2]^{1/2} = A_2/a_1 \tag{17}$$

is the body stability parameter. As depicted, this model assumes the control-surface actuator responds instantaneously to a command (i.e. possesses infinite slew-rate) but has a

Table 3 Transfer functions, coefficients, and constants for a typical ship

Nondimensional Coefficients		
$N_{\delta_r}' = -0.022$		$N_r' = -0.067$
$Y_{\delta_r}' = -0.046$		$Y_r' = -0.0875$
$N_\beta' = 0.108$		$Y_{\dot\psi}' = 0.072$
$Y_\beta' = -0.27$		$m_T' = 0.33$
	$I_{zz}' = 0.0215$	
Vehicle constants		
$H = 26.7$ ft	$\Delta = 35°$	$l = 500$ ft
Transfer functions azimuth plane		
$\psi/\delta_r = -1.0\ (s+1.5)/s(s+0.41)(s+3.6)$		
$\beta/\delta_r = -0.14\ (s+4.7)/(s+0.41)(s+3.6)$		
$y_0/\delta_r = -0.14\ (s+2.3)(s-4.8)/s^2(s+0.41)(s+3.6)$		

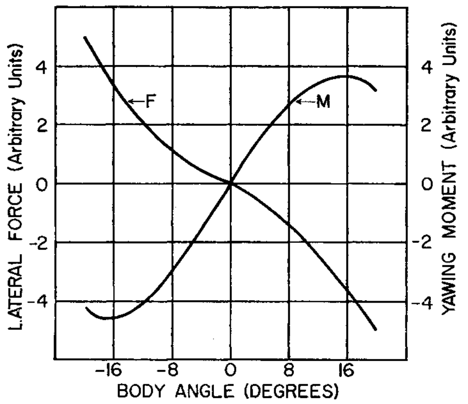

Fig. 4 Hydrodynamic force and moment vs vehicle sideslip angle (towing tank data).

maximum allowable deflection (position saturation), Δ. Experimental studies of the nonlinear behavior on simulated models and phase-plane analysis[10] of a simplified model indicate that the effects of the terms $s + a_T/s + a_1$ and $s + a/s + a_T$ upon dynamic behavior in turns are generally negligible. That is, because the nonlinearities limit the vehicle's motion, the frequencies involved in executing a turn are quite low, and in the range of interest $s + a_T/s + a_1 \approx a_T/a_1$ and $s + a/s + a_T \approx a/a_T$. Employing this approximation results in the simplified form of the normalized model shown in Fig. 6b where

$$J = -a_1/K_{\dot\psi}a \tag{18}$$

(a constant representing the effective normalized inertia),

$$k = Y_{|\beta_T|\beta_T}'(K_{\beta_T}a_T)^2/Y_{\delta_r}'K_{\dot\psi}aa_1 \tag{19}$$

and $Y_{|\beta_T|\beta_T}'$ is a constant whose value is dependent on the vehicle turning properties.

This modeling neglects the effect of time lags in the build-up of hydrodynamic forces and moments acting on the vehicle body and control surfaces. Empirical studies have shown that the response of the hydrodynamic force to a sudden rudder deflection is a function of the distance traveled in control surface chord lengths. The time constant associated with this lag, which has generally been assumed to be the time required to travel approximately three chord lengths, is sufficiently small so that its effect on vehicle turning is negligible. Typically, its effect is less significant than that of the $s + a_T/s + a_1$ and $s + a/s + a_T$ terms considered previously. For the hydrodynamic forces and moments acting on the body, where the effect of the hydrodynamic transient is less well known, it is not clear from estimates of the time constant that the corresponding time lag has a negligible hydrodynamic effect. However, actual vehicle responses tend to justify neglecting the combined effects of this lag and those previously discussed. Typical phase-plane trajectories of the error sig-

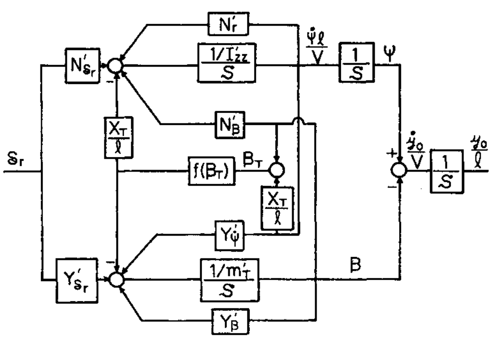

Fig. 5 Velocity-length normalized model of vehicle including nonlinear lift force.

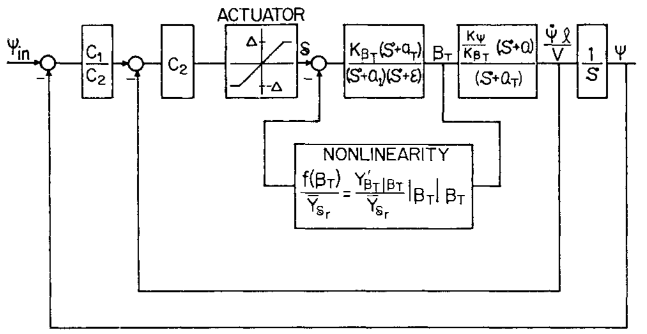

Fig. 6a Reduced velocity-length normalized model of azimuth dynamics.

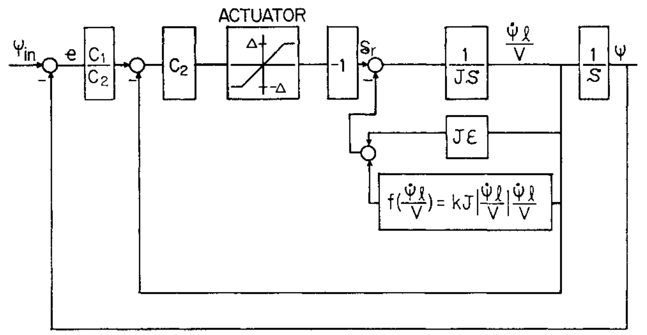

Fig. 6b Simplified model of azimuth dynamics.

nal, $e = \psi_{in} - \psi$, for the simplified model with the linear controller illustrated in Fig. 6b, are shown in Fig. 7. These trajectories essentially duplicate those of the full dynamics given in Fig. 5.

The effect of varying the controller constants for large step changes in heading is reflected primarily in the slope $-c_1/c_2$ of lines forming the boundary of the region of linear operation. Outside this linear region the rudder is at its maximum $\pm$ deflection. The desired large signal response is obtained by properly setting the ratio c_1/c_2. The gain c_2 is then adjusted on the basis of the linear (coursekeeping) model to yield good response for small signal inputs.

Turning Model with Restricted Rudder-Rate

The above control analysis, performed on the nonlinear body model with rudder position saturation, assumed rudder slew-rates large enough so as to be considered infinite. In high-performance vehicles, the restricted maximum slew-rate, inherent in all physical actuators, can become an important factor. Its effect on the turning qualities of the vehicle and in modifying the control laws derived previously is now considered.

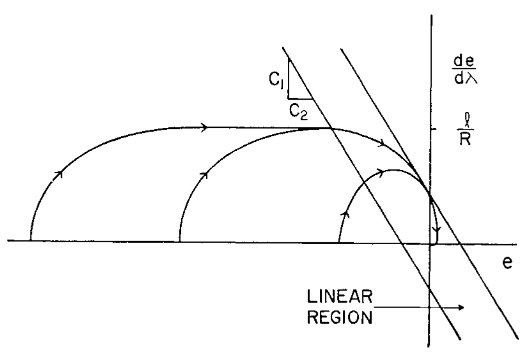

Fig. 7 Phase plane trajectories for simplified azimuth angle model.

The simplified model of the azimuth plane dynamics, employing a quadratic lift-force nonlinearity, is redrawn in Fig. 8a with an actuator model that includes limitations typical of steering gear. The actuator model consists of an integrator and two nonlinearities. The saturation in the forward transmission path represents the slew-rate limitation and the nonlinear feedback realizes the control-surface deflection (position) limitation, Δ. The magnitude of the slew-rate limitation, Ω, is modified by l/V to make the actuator consistent with the velocity-length normalized body model. As illustrated in the hard-over to hard-over maneuver of Fig. 1, the effect of a small value of Ω is to degrade the ship response. With actuator requirements increasing rapidly with increased slew-rate, some optimum value exists beyond which the added cost of realizing larger rates is not justified by the corresponding improvement in response.

Isolation of the effect of rudder-rate on system behavior is desirable and is achieved in this reduced model by introducing a new nondimensional time variable

$$\tau = [(\Delta/J)(R/l)][Vt/l] = [(\Delta/J)(R/l)]\lambda \quad (20)$$

Noting from Fig. 8a that $(\Delta/J)(V/l)^2$ is the maximum angular acceleration induced by rudder action, Eq. (20) may also be cast as

$$\tau = (\Delta/J)(V/l)^2(R/V)t = (\ddot{\psi}_{\max}/\dot{\psi}_{\max})t \quad (21)$$

where $\dot{\psi}_{\max} = V/R$ is the maximum turning rate of the vehicle. The operator corresponding to Eq. (20) is

$$S = (\dot{\psi}_{\max}/\ddot{\psi}_{\max})s = s/[(\Delta/J)(R/l)] \quad (22)$$

Inserting the operator S into Fig. 8a and performing some block diagram manipulation, the model of Fig. 8b results,

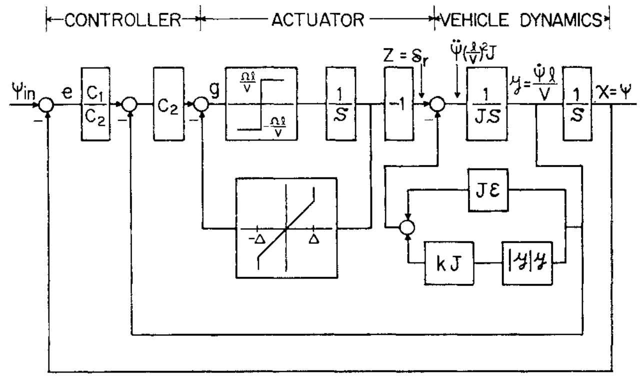

Fig. 8a Simplified azimuth model including limitations on actuator position and slew-rate.

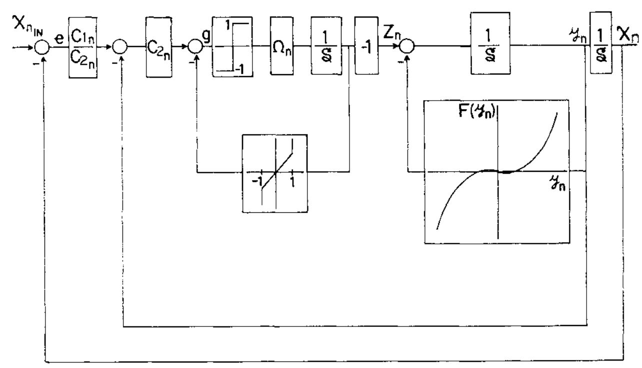

Fig. 8b Normalized nonlinear turning model; for the quadratic approximation to the hydrodynamic nonlinearity, $F(y_n) = [\epsilon/(\Delta/J)(R/l)]y_n + [K/(\Delta/J)(R^2/l^2)]|y_n|y_n$.

where

$$\Omega_n = (\Omega/\Delta)l/V/[(\Delta/J)(R/l)] \tag{23}$$

the states x_n, y_n, and z_n are related to those of the velocity-length model of Fig. 8a by

$$x_n = [(\Delta/J)(R/l)](R/l)x = [(\Delta/J)(R/l)](R/l)\psi \tag{24}$$

$$y_n = y(R/l) = R(\dot{\psi}/V) \tag{25}$$

$$z_n = z/\Delta = \delta_r/\Delta \tag{26}$$

and the controller gains relate to those of Eq. 13 by

$$c_{1n} = [(l/R\Delta)/(\Delta/J)(R/l)]c_1 \tag{27}$$

$$c_{2n} = (l/R\Delta)c_2 \tag{28}$$

In a steady turn, the signal transmission from $-z_n$ to y_n in Fig. 8b is the quadratic approximation to the normalized (turning rate)/(rudder deflection) characteristic of Fig. 3, that is

$$-z_n = F(y_n) = [\epsilon/(\Delta/J)(R/l)]y_n + [K/(\Delta/J)(R^2/l^2)]|y_n|y_n \tag{29}$$

The linear hydrodynamic feedback defines the initial slope of the characteristic, see Fig. 3, while the function of the quadratic term is to limit the normalized turning rate to $y_n = 1$. If the actual turning characteristic is used, the resulting "nonlinear turning model" of Fig. 8b accurately reproduces the steady turning behavior of the vehicle. The preceding development serves to establish the relationship of the "nonlinear turning model" to the linear coursekeeping model.

Effects of Restricted Rudder Rate on Turning Performance

For a given turning characteristic, the only parameter that appears in the above turning models is the normalized rudder rate Ω_n of Eq. (23). Therefore, the effect of a finite slew-rate on turning behavior can be readily examined by varying Ω_n and observing changes in the response for any of the standard maneuvers, e.g. the "hard-over to hard-over" sequence. This Paper uses a step change in heading and variations in response time for optimal execution of the maneuver as the criteria by which the effect of Ω_n is evaluated. The typical minimal time behavior of the system to a step command in azimuth angle, where the rudder is driven at maximum rate from one position limit to the other, is shown in Fig. 9. Note that the maneuver up to time t_2 is identical to the "hard-over to hard-over" maneuver and similar to the first two rudder executions of the "Z" maneuver. The azimuth angle response is seen to be clearly dependent on the size of the heading command, but because saturation of the vehicle turning rate occurs for a command of any significant size, removal of this dependency is possible. This is achieved by considering the time it takes to enter a turn (as defined by the time required to achieve 90% of the maximum turning rate) and the time to exit from a turn. With reference to Fig. 9,

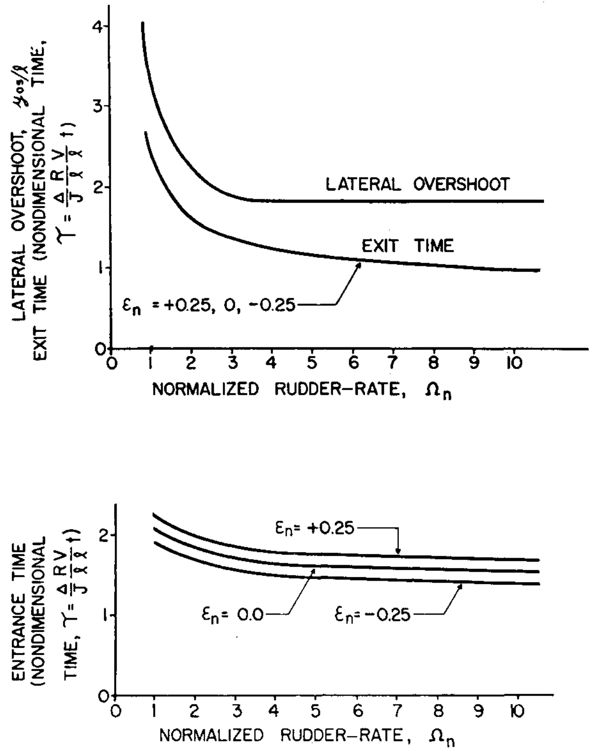

Fig. 10 Turning performance as measured by exit and entrance time vs normalized rudder-rate for various stability indices; lateral overshoot from Fig. 1b is replotted vs normalized rudder-rate for comparison with exit behavior.

$$t_{\text{exit}} = t_f - t_1 = t_3 - t_2 + (3/\Omega_n) \tag{30}$$

To obtain the time interval $t_3 - t_2$ an iteration procedure is used. Since $y_n(t_f) = 0$, $t_f - t_3 = 1/\Omega_n$ and the behavior of z_n is known, $y_n(t_3)$ can be determined. The assumptions of a saturated turning rate $y_n(t_1) = 1$ and the rudder being slewed at maximum rate for the period $t_2 - t_1 = 2/\Omega_n$ permit $y_n(t_2)$ to be calculated. Therefore, the determination of $t_3 - t_2$ becomes a boundary-point problem of matching the initial condition, $y_n(t_2)$, with the end condition, $y_n(t_3)$, for $z_n(t) = -1$. Assuming a quadratic hydrodynamic nonlinearity, with $|y_n|_{\max} = 1$ (see Fig. 8b), the nonlinear turning characteristic is completely defined by the body stability parameter ϵ. Therefore, the end points $y_n(t_2)$ and $y_n(t_3)$ become a function of Ω_n and $\epsilon_n = \epsilon/[(\Delta/J)(R/l)]$. By iteration methods the duration $t_3 - t_2$ was determined on the digital computer for various values of Ω_n with ϵ_n as a parameter. A plot of exit time, as defined in Eq. (30), is shown in Fig. 10a vs the normalized rudder-rate for a stable ($\epsilon_n = 0.25$), neutrally stable ($\epsilon_n = 0$), and unstable ($\epsilon_n = -0.25$) body configuration. The time required for a vehicle to enter a turn (i.e. the time to achieve 90% of maximum turning rate) was also determined numerically and is plotted in Fig. 10b.

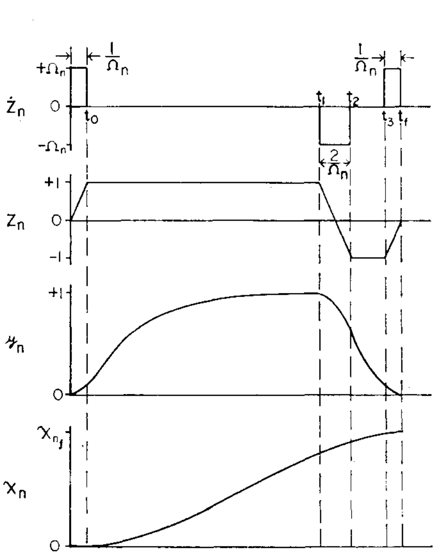

Fig. 9 Typical time optimal system response to step commands in azimuth angle.

Figures 10a and 10b clearly show the tradeoff between actuator requirements and turning performance as measured by the time to enter and/or exit a turn. Satisfactory operation is seen to result for values of $\Omega_n > 5$ although for vehicles

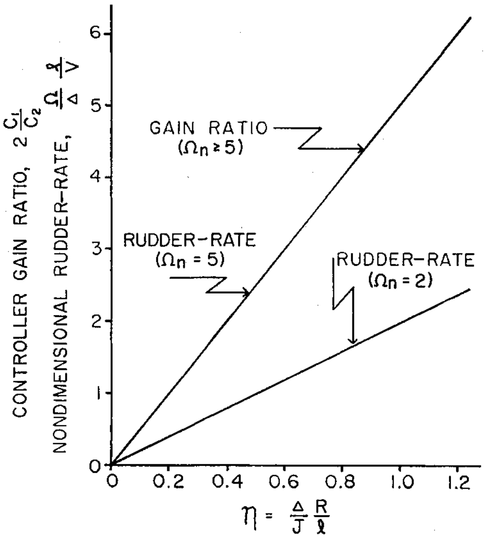

Fig. 11 Required nondimensional rudder-rate (for Ω_n = 2, 5) and controller gain ratio (for $\Omega_n > 5$) vs the reciprocal of the effective vehicle time constant or the elementary vehicle parameter, $\eta = (\Delta/J)\ (R/l)$.

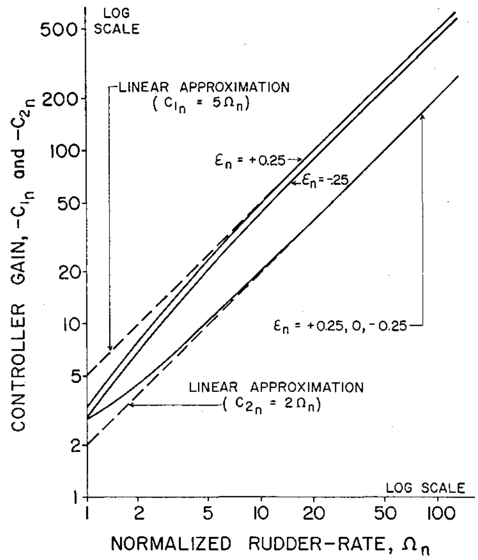

Fig. 13 Variation of controller gains c_{1n} and c_{2n} with normalized rudder-rate.

where a high degree of maneuverability is not required, designers may choose to operate at values as low as $\Omega_n = 1.5$ to 2.0. A curve of required rudder-rate (for values of $\Omega_n = 2$ and $\Omega_n = 5$) versus the vehicle parameter

$$\eta = (\Delta/J)(R/l) \tag{31}$$

is given in Fig. 11 and represents one of the major results of the paper. The reciprocal of η also represents an equivalent, or effective, time constant of the vehicle body dynamics. For the high-performance, torpedo-shaped submersible of Table 2 with $R/l = 5$ and a maximum operating speed of 20 knots, $\eta = 0.60$ and the desired rudder-rate ($\Omega_n = 5$) is $\Omega \cong 175°$ per sec. Similarly, for the ship of Table 3 with a maximum speed of 15 knots and $R/l = 3$, $\eta = 0.79$ and $\Omega = 6.9°$ per sec. To obtain a rudder-rate as low as the value of $2\frac{1}{3}°$ per sec, cited for a ship's rudder-rate in the introduction, requires operation at $\Omega_n = 1.7$, a value that is seen to press quite heavily on the border of acceptable performance. Since the effect of rudder-rate on turning performance is dominated by the exit behavior and the lateral overshoot in a hard-over to hard-over maneuver is roughly a measure of the exit behavior, the curve in Fig. 1b is superimposed on Fig. 10a for purposes of comparison. These analytically derived results, dependent only on knowledge of the elementary parameters J, Δ, and R/l, are seen to be consistent with those determined experimentally. While the goal of this research was the development of specifications for rudder-rates in high-performance submersibles, Fig. 11 provides a more meaningful relation between a vehicle and the required rudder-rate than that prescribed by present American Bureau of Shipping Rules. The latter have been previously shown to be unduly harsh on long, low-speed ships such as super tankers and insufficient for high-speed vessels.[1,7]

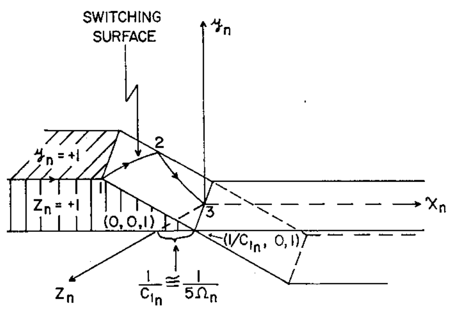

Fig. 12 State space diagram of normalized turning model showing piecewise linear approximation to optimal switching surface.

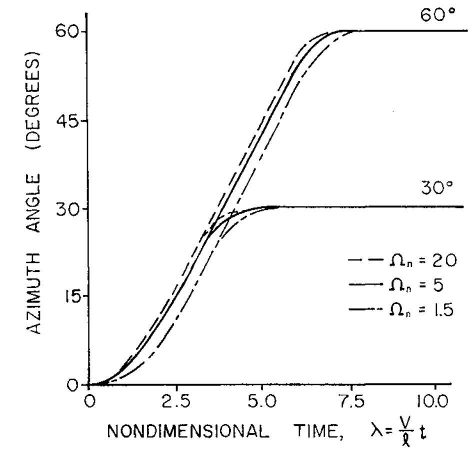

Fig. 14a Azimuth angle response for optimal setting of controller gains.

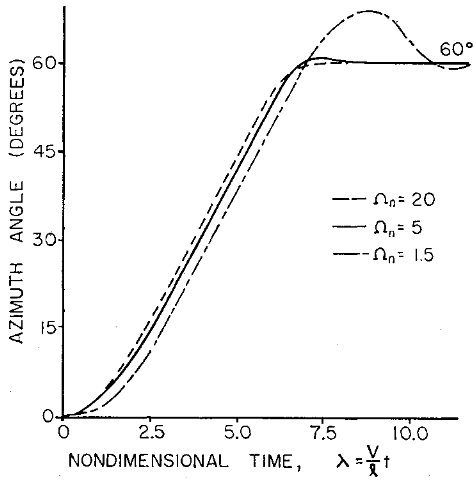

Fig. 14b Azimuth angle response for controller gains determined on the basis of infinite rudder-rate.

Azimuth Angle Controller for Vehicles with Limitations on Rudder Position and Slew-Rate

The controller gains in Fig. 8b necessary to achieve the optimal vehicle behavior illustrated in Figs. 9 and 10 remain to be obtained. Because of the body and actuator nonlinearities, the values that the normalized states y_n and z_n may attain are limited to the region $|z_n| \leq 1$ and $|y_n| \leq 1$ in the phase-space of Fig. 12. There are three points of interest (labeled 1, 2, and 3) in this diagram. Point 3 is the origin and is the desired final position of the state vector. Points 1 and 2 are the two switching points necessary to attain time optimal response for exiting, when the vehicle is turning at its maximum rate. These three points serve to define a plane that is assumed to be a satisfactory approximation to the optimal switching surface. This approximate switching surface is realized by the linear controller of Fig. 8b.

The feedback gains c_{1_n} and c_{2_n}, defined by the slope of the line formed by the intersection of the switching plane and the $x_n y_n$ plane, may be determined by setting the feedback signal equal to zero at the switching times t_1 and t_3. At time t_1, the feedback signal is given by

$$g(t_1) = c_{1_n}[x_n(t_f) - x_n(t_1)] - c_{2_n}[y_n(t_1)] - z_n(t_1) \quad (32)$$

and since $g(t_1) = 0$, $y_n(t_1) = 1$, and $z_n(t_1) = +1$, Eq. (32) reduces to

$$c_{1_n}[x_n(t_f) - x_n(t_1)] - c_{2_n} - 1 = 0 \quad (33)$$

Similarly, for $t = t_3$ we have

$$c_{1_n}[x_n(t_f) - x_n(t_3)] - c_{2_n} y_n(t_3) + 1 = 0 \quad (34)$$

Simultaneously solving Eqs. (33) and (34) for c_{1n} and c_{2n} yields

$$c_{1_n} = [1 + y_n(t_3)]/[y_n(t_3)\Delta x_n(t_1) - \Delta x_n(t_3)] \quad (35a)$$

and

$$c_{2_n} = \frac{\Delta x_n(t_1) - \Delta x_n(t_3)}{y_n(t_3)\Delta x_n(t_1) - \Delta x_n(t_3)} \quad (35b)$$

where $\Delta x_n(t_i) = x_n(t_f) - x_n(t_i)$. The values of $\Delta x_n(t_1)$, $\Delta x_n(t_3)$, and $y_n(t_3)$ were determined with the numerical procedure previously used in obtaining the exit time from a turn. The gains c_{1_n} and c_{2_n} are plotted versus Ω_n in Fig. 13. For the desired operating range of high-performance vehicles ($\Omega_n > 5$) these curves are approximated by

$$c_{1_n} \cong -5\Omega_n \quad (36a)$$

$$c_{2_n} \cong -2\Omega_n \quad (36b)$$

Substituting Eqs. (36a) and (36b) into Eqs. (27) and (28), the required gains for the velocity-length normalized system (see Figs. 6b and 8a) are found to be

$$c_1 = -5(\Omega/V/R) = -5\Omega/\dot{\psi}_{\max} \quad (37a)$$

$$c_2 = -(2\Omega R/V)/[(\Delta/J)(R/l)] = -2(\Omega/\dot{\psi}_{\max})\cdot 1/\eta \quad (37b)$$

Since the curves in Fig. 13 exhibit little change for different values of ϵ_n, Eqs. (37a) and (37b) are essentially independent of the vehicle body stability. Further, the ratio

$$c_1/c_2 = (5/2)(\Delta/J)(R/l) \quad (38)$$

valid for all $\Omega_n > 5$, is that which would result using infinitely fast slewing rates. For the submersible and ship considered earlier, the ratio in Eq. (38) is 1.5 and 2.2, respectively. The result of 1.5 is in close agreement with the value of 1.8 derived from in-water tests conducted on various torpedo-shaped submersibles. The somewhat higher value of this experimentally determined ratio is partially explained by the preference of the designers to have the actual angle response exhibit a slight overshoot.

Since both c_1/c_2 and Ω are defined by the parameter $\eta = (\Delta/J)(R/l)$, Eq. (38) is also plotted in Fig. 11 and represents the second major result of the paper.

Summary and Discussion

The nonlinear body model of Fig. 5 is adequate to determine both course-keeping and turning qualities of a moderately maneuverable ($R/l > 3$) submersible or floating vehicle. Under the assumptions leading to the simplified model of Figs. 6b and 8a, the only information required to determine the turning performance and desired controller constants is a knowledge of the vehicle velocity V, minimum turning radius R, or maximum turning rate $\dot{\psi}_{\max}$, vehicle length l, the vehicle constant J, and the rudder position and rate limitations, Δ and Ω. Figures 10a and 10b show the tradeoff between response time and rudder-rate, while Fig. 13 gives the values of the controller gains necessary to realize the indicated performance.

Note that both the required rudder-rate and controller gain ratio [see Eqs. (23) and (38)] depend on the elementary vehicle parameter $(\Delta/J)(R/l)$. This dependency, which represents the two major results of the paper, is plotted in Fig. 11. Simulation studies of both the simplified model of Fig. 8a and the full velocity-length normalized model of Fig. 5 were performed on the submersibles of Table 2 under restricted rudder slew-rate with rudder position saturation set at 30°. Figure 14a shows the optimal vehicle response to two different sized input commands for normalized rudder-rates of $\Omega_n = 1.5$, 5, and 20. This curve clearly shows the effect restricted control-surface slew-rate has on heading-change responses. Further, the results of the full vehicle dynamics in this simulation produced responses in close agreement with those of the simplified model, demonstrating the adequacy of the simplified model in defining control laws for moderately maneuverable hydrodynamic vehicles.

When the normalized slewing-rate is large the intersection of the switching plane with the $x_n z_n$ plane in the state space diagram of Fig. 12 approaches the z_n axis as $\Omega_n \cong c_{1_n}/5$ becomes large. If the value of Ω_n at which the vehicle is operating is sufficiently large, the change in the orientation of the plane for $\Omega_n = \%$ and that illustrated in Fig. 12 is small. Consequently, the difference in performance for a controller designed assuming infinite rudder-rate and that designed to achieve the switching surface is small. Further, the effect of the time lag in the build-up of the hydrodynamic forces on the control surface tends to render invalid the advantages of arbitrarily large rudder-rates. The desired range of operation indicated earlier ($\Omega_n \approx 5$) corresponds to slew-rates sufficiently fast to be assumed infinite and the control problem reduces to that first described with relation to Fig. 6b.

Figure 14b shows the responses of the vehicle for three finite values of rudder-rate ($\Omega_n = 1.5$, 5, and 20) when the controller design, as described above, was based on infinite rudder-rate. Satisfactory response is observed for $\Omega_n > 5$ with increased overshoot occurring as the value of Ω_n is decreased.

Inherent in the above development is the assumption of constant vehicle speed. While such an assumption is reasonable under coursekeeping conditions, a reduction in speed of about 25% is observed in a standard Z-maneuver.[1] However, this speed change is reasonably slow compared to the time constants of the full vehicle dynamics and, consequently, permit the use of integrated vehicle velocity to define distance traveled in vehicle lengths.

Conclusions

The intent of this paper, to simplify the representation of moderately maneuverable ($R/l > 3$) vehicles consistent with observed behavior, was realized. The critical factors affecting control and turning performance were identified and practical parametric relations developed. Linear feedback of the velocity-length normalized states ψ and $\dot{\psi}(l/V)$ was shown to provide satisfactory yaw angle control for both large and small heading changes. This velocity-adaptive control law requires minimal hardware and is readily implemented by modifying the gain in the rate gyro-loop with vehicle speed. For vehicles with low rudder-rates the relation between turning time and rudder-rate is displayed in Fig. 10. The finite slewing rate of the steering gear was shown to have little effect on maneuverability for normalized values of $\Omega_n = [(\Omega/A)/\eta](l/V)$ greater than 5. Design values of the required rudder-rate and controller gain ratio are given in Fig. 11 in terms of the vehicle constant $\eta = \Delta/JR/l$.

Finally, while this paper demonstrates that a precise model is not necessary to obtain meaningful results, such efforts should not supersede the continuing studies directed at refining dynamic models of floating and submerged vehicles.

In particular, this study does not consider the unique problems of vehicles with large rudders or highly maneuverable vehicles ($R/l = 1.5$) with special auxiliary equipment capable of producing additional turning forces, where precise knowledge of vehicle hydrodynamics is essential to the development of useful control systems.

References

[1] Eda, H. and Crane, L. C., "Steering Characteristics of Ships in Calm Waters and Waves," Annual Meeting of Society of Naval Architects and Marine Engineers, New York, 1965.

[2] Chen, H.-H., "Some Aspects of Ship Maneuverability," *Journal of Ship Research*, June 1969, Vol. 13, No. 2, pp. 111–128.

[3] Goclouski, J. and Gelb, A., "Dynamics of an Automatic Ship Steering System," *IEEE Transactions on Automatic Control*, Vol. AC-11, July 1966.

[4] Gertler, Morton, "The DTMB Planar-Motion-Mechanism System," *Symposium on Towing Tank Facilities, Instrumentation, and Measuring Techniques*, Zagreb, Yugoslavia, Sept. 1959, Dept. of Navy Rept., David Taylor Model Basin, Washington, D.C.

[5] Suarez, A., "Rotating Arm Experimental Study of Marine Class Vessels," 10th International Towing Tank Conference, 1963; also Suárez, A. and Breslin, J., "Davidison, Laboratory Rotating Arm Facility," DL Note 597, 1960, Stevens Institute of Technology, Hoboken, N.J.

[6] Lindgren, A. G., Cretella, D. B., and Bessacini, A. F., "Dynamics and Control of Submerged Vehicles," *ISA Transactions*, Vol. 6, No. 4, Dec. 1967, pp. 335–346.

[7] Yamamoto, Heiya, "A Tentative Theory on a Determination of the Power of a Main Steering Gear—On the Optimum Angular Velocity of a Main Steering Gear," *Journal of Society of Naval Architects of Japan*, Vol. 121, June 1967.

[8] Nomenclature for Treating the Motion of a Submerged Body through a Fluid," Report of the American Towing Tank Conference, Society of Naval Architects and Marine Engineers, New York, April 1950, pp. 5–15.

[9] Bottacini, M. R., "The Stability Coefficients of Standard Torpedos," Rept. 3345, July 1954, Naval Ordnance Lab., Silver Spring, Md.

[10] Graham, D. and McRuer, D., *Analysis of Nonlinear Control Systems*, Wiley, New York, 1961, pp. 272–433.

[11] Lindgren, A. G. and Cretella, D. B., "Effect of Restricted Rudder-Rate on the Turning Characteristics and Control of Submerged Vehicles," Rept. 417-02, May 1968, Div. of Engineering Research and Development, Univ. of Rhode Island, Kingtson, R.I.

[12] Vaughan, D. R. and Foster, W. C., "Feedback Designs of Systems with Saturation Constraints," *ISA Transactions*, Vol. 5, April 1966.

OCTOBER 1971 J. HYDRONAUTICS VOL. 5, NO. 4

Hydrodynamic Resistance of Towed Cables

YOUNG-IL CHOO* AND MARIO J. CASARELLA†

The Catholic University of America, Washington, D. C.

The hydrodynamic resistance on a towing cable is formulated on the basis of the independence principle which deduces that the chordwise viscous flow around a yawed cylinder is independent of the spanwise flow. The total resistance is resolved into the normal and the tangential resistances, respectively normal and tangential to the cable axis. The formulas of the normal and the tangential resistances can be universally applied to cables of any cross-sectional shape, and, for a given shape, require some empirical relationships that can be directly and conveniently obtained with a minimum of testing in a wind tunnel. This feature is attributable to the fact that the normal and the tangential resistances are expressed solely as functions of the Reynolds number based on the velocity component perpendicular to the axis of the cable. Working formulas for circular cables, derived from the universal formulas, yield values of the resistances that agree well with limited experimental data.

Nomenclature

C_D = drag coefficient, Eq. (4)
$[C_D]_f$ = frictional-drag coefficient
$[C_D]_p$ = pressure-drag coefficient
D = total drag per unit length of cable (or cylinder) oriented perpendicular to stream
d = diameter of circular or stranded cable in unstrained state
$\mathbf{e}_1,\mathbf{e}_2,\mathbf{e}_3$ = unit vectors in the z_1-, z_2-, z_3-directions, respectively
$\mathbf{f}_f,\mathbf{f}_p$ = frictional and pressure resistances, respectively, per unit material length of cable
$\mathbf{f}_n$ = $f_n\mathbf{n}$, normal resistance per unit material length of cable
$\mathbf{f}_\tau$ = $f_\tau\boldsymbol{\tau}$, tangential resistance per unit material length of cable
h_1,h_2,h_3 = scale factors of z_1,z_2,z_3, respectively, Eq. (23)
h = local heat-transfer coefficient of fluid, Eq. (35)
$\bar{h}$ = average heat-transfer coefficient, Eq. (37)
k = thermal conductivity of fluid
L = characteristic length of cable
L_c = circumference of the cross section of cable, Eq. (38)
$\mathbf{n}$ = unit vector normal to the cable, Fig. 1
Nu = $\bar{h}L/k$, average Nusselt number
p = fluid pressure
Pr = $\mu c_p/k$, Prandtl number, where c_p is specific heat of fluid at constant pressure
$\mathbf{q}$ = heat-transfer rate per unit area
Re = $\rho LW/\mu$, Reynolds number
Re_n = $Re\cdot\sin\phi$
s = material coordinate, representing the arc length between the lower-end point and a material point P of cable in unstrained state
T = temperature in two-dimensional flow

Received September 21, 1970; revision received April 30, 1971.

* Research Associate, Institute of Ocean Science and Engineering.

† Associate Professor of Mechanical Engineering, Institute of Ocean Science and Engineering. Member AIAA.